

Paolo Marocco¹, Maria Chiara Massaro², Alessandro Hugo Antonio Monteverde², Massimo Santarelli¹

¹Department of Energy, Politecnico di Torino, Corso Duca degli Abruzzi 24, 10129 Torino, Italy ²Department of Applied Science and Technology, Politecnico di Torino, Corso Duca degli Abruzzi 24, 10129 Torino, Italy

Abstract

Decarbonisation is a major challenge for the aviation sector, necessitating a radical shift and the exploration of innovative solutions to mitigate its environmental impact. In this context, hydrogen-powered fuel cells have gained significant attention in recent years due to their capacity to eliminate carbon dioxide emissions during flight. This study aims to investigate the effectiveness and main barriers of using low-temperature PEM fuel cells in aviation. A design methodology is applied to derive the weight-optimal design of several hydrogenpowered configurations. For each configuration, a minimum-weight layout is derived by accurately estimating the weights of the main components involved in the propulsion system, including hydrogen storage, fuel cell stack and related auxiliaries. The analysis is specifically applied to a regional passenger aircraft, namely the ATR 72-600. Additionally, the technical viability of the fuel cell-based aircraft is explored by comparing its maximum take-off weight (MTOW) with that of the conventional kerosene-based layout. This study demonstrates that across all the examined scenarios, oversizing the number of fuel cell stacks emerges as a weight-optimal solution, as the resulting higher efficiency reduces both the hydrogen consumption and the heat generated during fuel cell operation. In particular, the weight-optimal number of stacks increases when considering hydrogen storage technologies characterised by low gravimetric density. It is also highlighted the need of decreasing the weight of both the hydrogen storage and the cooling system to enhance the competitiveness of the hydrogen-based solution in terms of weight compared to the kerosene configuration. Achieving gravimetric density values for hydrogen storage above approximately 15-20 wt% is crucial. Especially, future research should focus on the thermal management system, which can account for up to 50% of the total propulsion system weight.

Keywords: Hydrogen, Aviation, Fuel cell, All-electric aircraft, Decarbonisation

1. Introduction

Presently, aviation accounts for 12% of transport-related CO₂ emissions and approximately 5% of anthropogenic global greenhouse gas emissions. Despite measures have been taken over the past two decades to improve aircraft fuel efficiency, CO₂ emissions have continued to grow due to a constant increase in global aviation demand [1]. In particular, Airbus envisions a 4.6% per year growth in the annual global traffic rate for the period 2015-2034, while Boeing predicts a slightly higher rise over the same timeframe [2]. Therefore, promoting initiatives and developing new technologies to limit aviation's climate impact is of fundamental importance [3].

Within this framework, the concept of aircraft electrification has garnered significant attention from both academia and industry in recent years. This is testified by an ever-increasing number of studies on the topic and the establishment of numerous startup companies aiming to bring electric propulsion systems to the commercial market [4]. Electric powertrain layouts that rely entirely on batteries have been developed. However, their restricted endurance and significant weight currently make them unsuitable for long-range transport applications [5]. Recently, there has been growing interest in exploring the use of hydrogen combined with fuel cells as a potential solution for achieving a zero-emission all-electric aircraft configuration [6]. Alternatively, hydrogen can be employed for aircraft

propulsion through thermal conversion in combustion engines [7]. Moreover, hydrogen, when combined with carbon dioxide, can serve as a base for the synthesis of sustainable aviation fuels (SAFs) [8].

Despite the promising potential for decarbonising aviation, the technical feasibility of using hydrogen-powered fuel cells still requires thorough investigation. Massaro et al. [9] demonstrated that an all-electric aircraft based on low-temperature proton exchange membrane (PEM) fuel cells would currently weigh 25-50% more than a conventional kerosene-based aircraft. Solid oxide fuel cells (SOFCs) also possess interesting characteristics for aviation, such as fuel flexibility and high conversion efficiency, rendering them potentially viable for long-range flights [10]. Overall, an optimal design of the fuel cell system is crucial to ensure the technical feasibility of hydrogen-based solutions [11]. Additionally, it has been found that the electrochemical cell performance, which varies depending on the operating point of the fuel cell, should be considered during the design stage to achieve a configuration with minimal propulsion system weight [12].

The main objective of this work is to uncover the potential and current limitations of low-temperature PEM fuel cells for aviation applications. By further exploring the design methodology developed by the authors in a previous work [12], the performance map of the fuel cell is used to investigate several all-electric hydrogen-based configurations and, for each of them, derive a minimum weight layout of the propulsion system (encompassing hydrogen storage, fuel cell stack and related auxiliaries). Specifically, the maximum take-off weight (MTOW) of the innovative solution is determined through a detailed estimation of the weights of all components within the propulsion system. Particular attention is paid to identifying the components that exert the most significant influence in terms of weight. The technical viability of the hydrogen-based configurations is also assessed by computing the change in weight compared to a conventional kerosene-powered aircraft.

2. Materials and methods

The following sections outline the approach used for the design of a hydrogen-based propulsion system, as well as the methodology for estimating the MTOW. Additionally, the main input data required for the sizing process are provided.

2.1 Kerosene- and hydrogen-based propulsion systems

As shown in Figure 1, the use of fuel cells implies that some components of the conventional kerosene-based aircraft must be replaced. In particular, the kerosene storage system and the thermal engines are substituted with the hydrogen storage system, the fuel cell system (comprising the stack and related auxiliaries) and electric motors. The fuel cell unit is essential for converting hydrogen into electricity, while the electric motor allows electrical power to be turned into mechanical power.

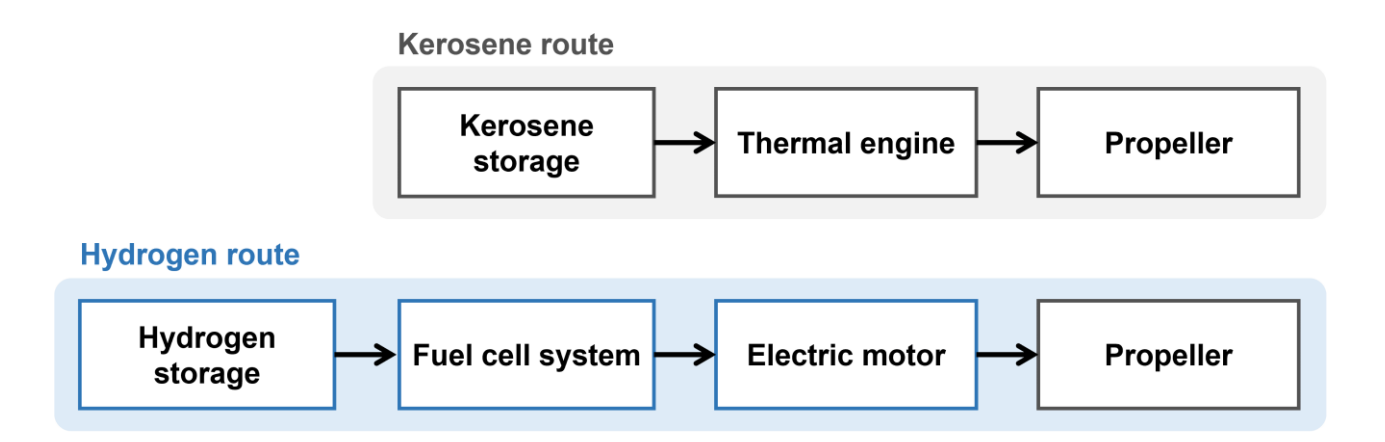


Figure 1 – General layout of the kerosene- and hydrogen-based propulsion systems.

The analysis is applied to the commercial aircraft ATR 72-600, which is currently powered by kerosene. Table 1 outlines the main features of a typical ATR 72-600 flight mission, including take-off and cruise power, total flight duration and maximum altitude [9].

Parameter	Value		
Take-off power (half-wing), P_{TO}	1,846 kW		
Cruise power (half-wing), P_{CR}	1,590 kW		
Flight duration	2 h		
Max altitude (cruise), h_{CR}	4,600 m		

Table 1 – Flight mission characteristics of the ATR 72-600.

2.2 Sizing of the hydrogen-based propulsion system

The aim of this section is to provide a methodology for designing a fuel cell-based propulsion system for aircraft applications, including the hydrogen storage, the fuel cell stacks and all the needed auxiliaries (mainly the cooling system and the air compressor).

2.2.1 Fuel cell stack

A stack manufactured by Ballard has been chosen for this study (FCgen®-HPS) [9]. The cell-level polarisation curve is shown in Figure 2, while its main technical features are detailed in Table 2.

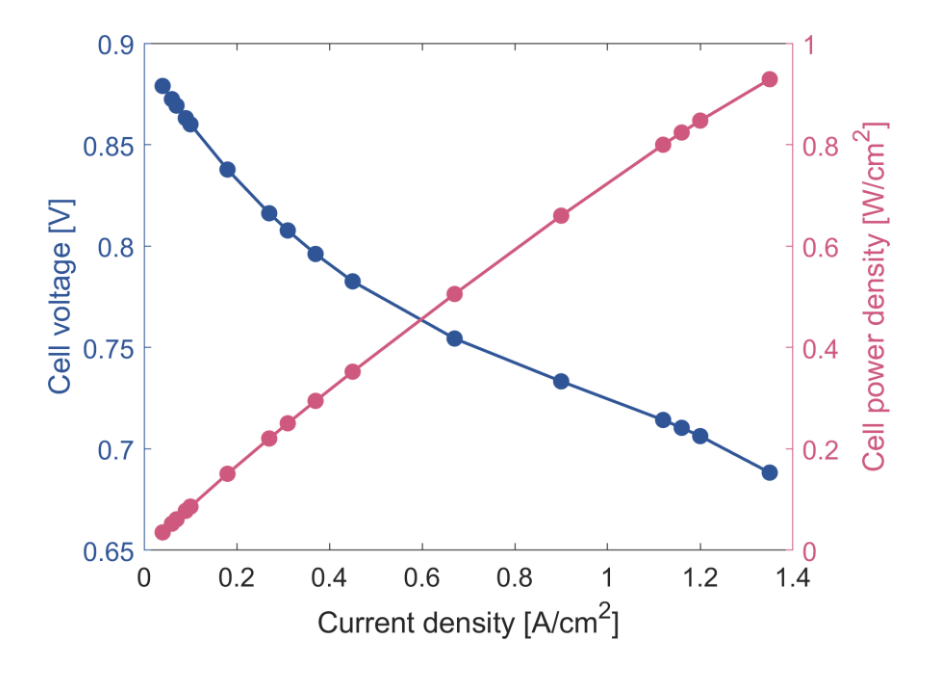


Figure 2 – Cell voltage (left) and cell power density (right) of FCgen®-HPS.

Parameter	Value		
Nominal stack power (gross), $P_{FC,stack,gross,nom}$	137.8 kW		
Nominal cell current density, i_{nom}	1.35 A/cm ²		
Cells per stack, n_{cell}	309		
Cell area, A_{cell}	480 cm ²		

Table 2 – Technical specifics of the fuel cell stack data (FCgen®-HPS).

For a given current density (i, in A/cm²), the gross electrical power generated by the fuel cell stack ($P_{FC,stack,gross}$, in kW) can be computed as:

$$P_{FC.stack.gross}(i) = i \cdot A_{cell} \cdot V_{cell}(i) \cdot n_{cell} \cdot 10^{-3}$$
(1)

where A_{cell} (in cm²) is the cell area, V_{cell} (in V) is the cell voltage and n_{cell} is the number of cells per

stack. The net electrical power exiting the fuel cell stack ($P_{FC,stack,net}$) can be then assessed by subtracting the electrical demand required by the auxiliary components:

$$P_{FC,stack,net}(i,h) = P_{FC,stack,gross}(i) - P_{AC,stack}(i,h) - P_{add,stack}$$
(2)

where $P_{AC,stack}$ (in kW) is the electricity consumed by the compressor to supply air to the fuel cell stack. It depends on the current density (i) and on the altitude (h), as shown by the following expression:

$$P_{AC,stack}(i,h) = \dot{m}_{air,stack}(i) \cdot c_p \cdot T(h) \cdot \left(\beta(h)^{\frac{\gamma-1}{\gamma}} - 1\right) \cdot \frac{1}{\eta_{is} \cdot \eta_{em}}$$
(3)

The term $\dot{m}_{air,stack}$ (in kg/s) is the air flow rate entering the stack (cathode side) and was computed based on the Faraday's law, c_p (in kJ/(kg·K)) is the specific heat capacity at constant pressure of air, T (in K) is the temperature of the air flow at the compressor inlet, β is the ratio between the cathode operating pressure (1.5 bar) and the external air pressure, γ is the heat capacity ratio of air, η_{is} (equal to 0.75) is the isentropic efficiency of the compressor and η_{em} (equal to 0.95) is the electro-mechanic efficiency of the compressor. The air properties (c_p and γ) were derived by employing temperature-dependent polynomial functions. The expressions to compute temperature and pressure of the outside air as a function of altitude can be found in [12].

In Eq. (2), $P_{add,stack}$ (in kW) is the power consumption of the other auxiliary components (small equipment such as pumps, valves, control unit). It was modelled as a constant term and assumed to be a fixed percentage (1%) of the nominal gross stack power [9].

The net electrical power of the fuel cell system ($P_{FC,stack,net}$, in kW) was then used to determine the number of stacks (n_{stack}) needed to consistently meet the power requirements of the flight mission. As shown in Eq. (4), the most demanding condition between take-off (TO) and cruise (CR) was chosen to select the required number of stacks.

$$n_{stack} = 2 \cdot max \left(\left[\frac{P_{TO}}{\eta_{EM} \cdot P_{FC,stack,net}(i, h_{TO})} \right], \left[\frac{P_{CR}}{\eta_{EM} \cdot P_{FC,stack,net}(i, h_{CR})} \right] \right)$$
(4)

where $\lceil x \rceil$ is the ceiling function that gives the smallest integer greater than or equal to x, P_{TO} (in kW) is the take-off power, P_{CR} (in kW) is the cruise power, η_{EM} is the electro-mechanical efficiency of the electric motor, h_{TO} is the take-off altitude and h_{CR} is the cruise altitude. The multiplication by two was done to obtain the total number of stacks, given that P_{TO} and P_{CR} are provided at half-wing level.

As an initial case, the nominal current density (i_{nom}) was used in Eq. (4) to evaluate the net fuel cell electrical power, resulting in a configuration with the fewest number of stacks. A sensitivity analysis was then performed by gradually decreasing the value of i to explore the potential benefits of oversizing the fuel cell system (i.e., increasing the number of stacks, allowing them to operate at partial loads). Operating the fuel cell stack at partial loads increases efficiency, which positively impacts the fuel storage (less hydrogen to be stored) and the cooling system (less heat to be removed). The goal is to identify the configuration that minimises the weight of the propulsion system (see Section 2.3), achieved through a trade-off between the number of fuel cell stacks and the size of both the hydrogen storage and the cooling system.

For a given number of stacks (n_{stack}) , the actual net power generated by the fuel cell system can be estimated for both take-off and cruise conditions according to the following expression (with j = TO, CR):

$$P_{FC,stack,net}(i_j, h_j) = 2 \cdot \frac{P_j}{\eta_{EM} \cdot n_{stack}}$$
 (5)

The actual operating current density during take-off (i_{TO}) and cruise (i_{CR}) can subsequently be estimated based on the net output power of the fuel cell $(P_{FC,stack,net})$ under those specific conditions. The net electrical efficiency of the fuel cell system (η_{net}) during take-off and cruise can also be assessed through Eq. (6) (with j=TO,CR):

$$\eta_{net}(i_j, h_j) = \frac{P_{FC, stack, net}(i_j, h_j)}{\dot{m}_{H2, stack}(i_j) \cdot LHV_{H2} \cdot 10^3}$$
(6)

where LHV_{H2} (in MJ/Kg) is the lower heating value of hydrogen and $\dot{m}_{H2,stack}$ (in kg/s) is mass flow rate of hydrogen required by the fuel cell. The latter term was calculated based on Faraday's law.

2.2.2 Cooling system

A cooling system is essential for managing the thermal power generated by the fuel cell stack. It consists of a closed circuit using a liquid coolant, assumed to be Glysantin, for cooling the stack. Additionally, an air radiator is included to restore the coolant to its initial temperature. The temperature variation of the liquid coolant was set to 10 °C, while that of the cooling air stream was set to 15 °C. The ε -NTU method was employed to estimate the nominal heat exchange area of the cooling system ($A_{CS,stack,nom}$, in m²) required to remove the heat generated by a single stack. All input parameters necessary for the cooling system design, along with an explanation of how to apply the ε -NTU method, are provided in [12].

It should be noted that the thermal power to be removed by the cooling system depends on the operating condition of the fuel cell. For both take-off and cruise, the heat produced per stack can be computed as follows (with j = TO, CR):

$$Q_{FC,stack}(i_j) = i_j \cdot A_{cell} \cdot \left(\frac{-\Delta \bar{h}_{react}}{2F} - V_{cell}(i_j)\right) \cdot n_{cell} \cdot 10^{-3}$$
(7)

where $Q_{FC,stack}$ (in kW) is the thermal power generated by the stack, $\Delta \bar{h}_{react}$ is the molar enthalpy of reaction (-285,829 J/mol) and F (in C/mol) is the Faraday constant. The larger of the two thermal power values (i.e. at TO and CR) was then considered for estimating the heat exchange area of the cooling system.

2.2.3 Air compressor

The electrical power required by the air compressor to supply air to a single stack was computed according to Eq. (3) for both take-off conditions (i_{TO} and h_{TO}) and cruise conditions (i_{CR} and h_{CR}). The maximum value between the two was then taken as the nominal power of the air compressor ($P_{AC.stack.nom}$, in kW).

2.2.4 Hydrogen storage

The amount of hydrogen fuel required to meet the power demand of the mission ($W_{H2,nom}$, in kg) can be expressed according to the following general relationship:

$$W_{H2,nom} = 2 \cdot \int_0^{t_{end}} \frac{P_{mission}(t)}{\eta_{EM} \cdot \eta_{net}(t) \cdot LHV_{H2} \cdot 10^3} dt$$
 (8)

where $P_{mission}$ (in kW) is the mechanical power required and t_{end} (in s) is the overall flight duration. Note that the expression in Eq. (8) is multiplied by two because $P_{mission}$ is provided at half-wing level. In this analysis, the hydrogen mass was derived considering a constant hydrogen flow rate throughout the mission, set equal to the amount required during the cruise phase [12]. Namely, P_{CR} was used as the mechanical power to be covered and η_{net} (net efficiency of the fuel cell system) was evaluated under cruise flight conditions according to Eq. (6). This approximation is reasonable since the cruise phase constitutes the majority of the flight time.

2.3 MTOW estimation

The maximum take-off weight of the kerosene-based aircraft ($MTOW_{KR}$, in kg) is:

$$MTOW_{KR} = W_{PR} + W_{ST} + W_{PL} + W_{ESPG,KR}$$
 (9)

where W_{PR} is the weight of the two propellers, W_{ST} is the weight of the aircraft structure, W_{PL} is the weight of the payload, and $W_{ESPG,KR}$ is the weight of the kerosene-based energy storage and power generation (ESPG) system. The latter term includes two thermal engines, the fuel storage tank and

the fuel. The values of all terms of Eq. (9) are displayed in Table 3.

Parameter	Value		
Maximum take-off weight, $MTOW_{KR}$	22,800 kg		
Propellers, W_{PR}	342 kg		
Structure, W_{ST}	10,479 kg		
Payload, W_{PL}	7,550 kg		
Energy storage and power generation, $W_{ESPG,KR}$	4,429 kg		

Table 3 – Weight values of the components included in the kerosene-based aircraft. Data refer to ATR 72-600 aircraft.

The MTOW of the innovative aircraft ($MTOW_{H2}$, in kg) can be derived similarly to Eq. (9), by replacing $W_{ESPG,KR}$ with the weight of the new ESPG system:

$$MTOW_{H2} = W_{PR} + W_{ST} + W_{PL} + W_{ESPG,H2}$$
 (10)

The term $W_{ESPG,H2}$ encompasses the hydrogen storage system (including the hydrogen fuel), the fuel cell system and the electric motors. Specifically, the fuel cell system includes the fuel cell stacks and all the needed auxiliaries (mainly the cooling system and the air compressor). Overall, the weight of the hydrogen-powered ESPG system can be expressed as follows:

$$W_{ESPG,H2} = GI_{CS} \cdot A_{CS,stack,nom} \cdot n_{stack} + \frac{W_{H2,nom}}{GI_{HS}} + \frac{2 \cdot P_{TO}}{\eta_{EM} \cdot GI_{EM}} + \frac{P_{FC,stack,gross,nom} \cdot n_{stack}}{GI_{FC,stack}} + \frac{P_{AC,stack,nom} \cdot n_{stack}}{GI_{AC}}$$

$$(11)$$

where GI_j is the gravimetric index of the j-th component, $A_{CS,stack,nom}$ (in m²) is the surface area of the heat exchanger involved in the cooling system, $W_{H2,nom}$ (in kg) is the mass of hydrogen consumed by the fuel cell during the mission, P_{TO} (in kW) is the take-off power of the flight mission (half-wing), η_{EM} (in %) is the electro-mechanical efficiency of the electric motor, $P_{FC,stack,gross,nom}$ (in kW) is the nominal power of a single fuel cell stack (gross power), n_{stack} is the number of fuel cell stacks and $P_{AC,stack,nom}$ (in kW) is the nominal power of the air compressor needed by a single stack.

The values of the gravimetric indexes, along with their respective units of measurement, are shown in Table 4 [12]. As regards the hydrogen storage component, a sensitivity analysis was conducted on the gravimetric index (i.e., gravimetric storage density) to explore the technical viability of several hydrogen storage technologies.

As described in Section 2.2.1, the number of fuel cell stacks (computed through Eq. (4)) was selected with the objective of minimising the weight of the fuel cell-based ESPG system (i.e. $W_{ESPG,H2}$, calculated by Eq. (11)).

Parameter	Value
Electric motor, GI_{EM}	5.2 kW/kg
Cooling system, GI _{CS}	1.08 kg/m ²
Air compressor, GI_{AC}	1.03 kW/kg
Fuel cell stack, $GI_{FC,stack}$	3 kW/kg
Hydrogen storage, GI_{HS}	Sensitivity analysis

Table 4 – Gravimetric index values of the main components involved in the hydrogen-based propulsion system. A sensitivity analysis was conducted on the gravimetric index of hydrogen storage (in wt%).

3. Results and discussion

Table 5 reports the sizing results for several hydrogen-based configurations, in which the hydrogen storage technology is varied. The values of gravimetric storage density for the different solutions were taken from [9].

As shown in Table 5, the MTOW ranges from 52.4 t (for low-temperature metal hydrides) to 29.7 t (cryo-compressed hydrogen), representing an increase of 130% to 30% compared to the kerosene-based solution. The weight of the ESPG system is also specified and ranges from 34.1 t to 11.3 t. For all configurations, the minimum number of fuel cell stacks is 30, as derived from Eq. (4) based on the nominal current density (i_{nom}) . It is noteworthy that the weight-optimal number of stacks always exceeds 30, allowing each stack to be operated at lower power during cruise and take-off. Despite the increased weight associated with additional stacks, the resulting higher efficiency is useful to reduce the size of both the hydrogen storage and the cooling system. Moreover, increasing the number of stacks is particularly advantageous for hydrogen storage typologies with low gravimetric storage density. In these cases, the weight fraction of the hydrogen storage increases, and operating at higher efficiency (thanks to the fuel cell oversizing) can help mitigate this effect. Specifically, the weight-optimal number of stacks decreases from 66 to 36 when the gravimetric storage density increases from 1.4 wt% (low-temperature metal hydride) to 8.5 wt% (cryo-compressed hydrogen).

Hydrogen storage typology	Gravimetric storage density [wt%]	Number of stacks [-]	ESPG mass [t]	MTOW [t]	MTOW change [%]
Low-temperature metal hydride	1.4	66	34.1	52.4	130.0
Liquid organic hydrogen carrier	4.1	40	16.3	34.6	51.9
High-temperature metal hydride	4.3	40	15.8	34.2	49.9
Metal organic framework	4.9	40	14.7	33.1	45.1
Compressed hydrogen (700 bar)	5.7	40	13.6	32.0	40.2
Liquid hydrogen	7.5	36	11.9	30.3	33.0
Metal borohydride	8.0	36	11.6	30.0	31.5
Cryo-compressed hydrogen	8.5	36	11.3	29.7	30.3

Table 5 – Weight-optimal sizing results for different hydrogen storage technologies. "MTOW change" is computed with respect to the kerosene-based configuration (whose MTOW is 22.8 t).

Figure 3 displays the weight contribution of the main components of the ESPG system for the hydrogen-based configuration: electric motor, hydrogen storage, fuel cell stacks and related auxiliaries (air compressor and cooling system). The black solid line indicates the ESPG weight for the hydrogen-based configuration, while the dashed black line corresponds to the kerosene-based solution (4.4 t).

As the gravimetric index of hydrogen storage increases from 2 to 30 wt%, the total ESPG weight reduces from 26 t to 8 t. It can be noted that hydrogen storage is the most significant contributor up to a gravimetric index of approximately 10 wt%. Beyond this value, the cooling system starts to account for the largest weight share (up to 50%), and the total ESPG weight decreases more gradually as the gravimetric index increases. Overall, the hydrogen-based ESPG system always weighs more than the conventional kerosene-based alternative, even when considering high values of gravimetric storage density (up to 30 wt%). This underscores the necessity of finding solutions to lower the weight of the fuel cell system, particularly the cooling equipment.

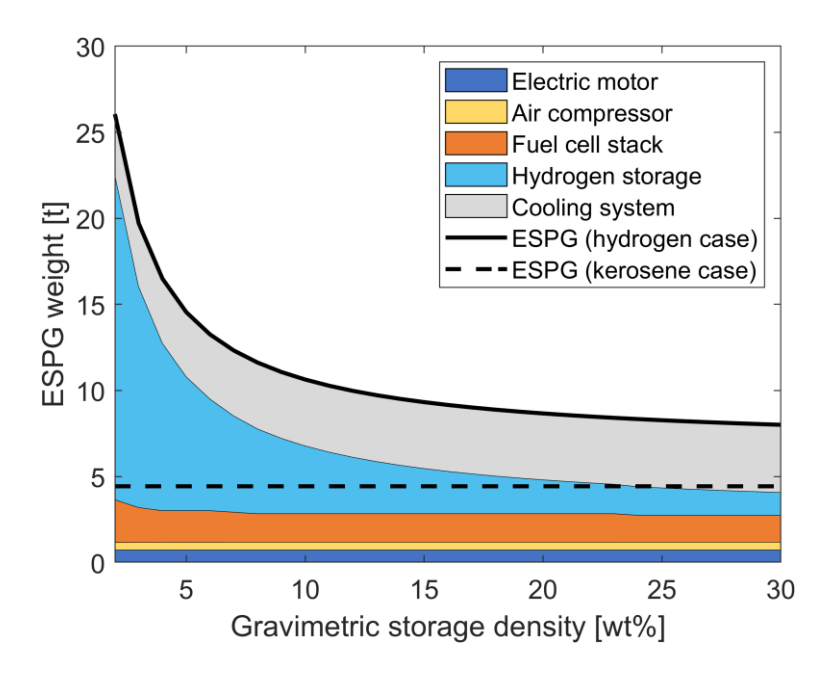


Figure 3 – ESPG weight of the hydrogen-based configuration (solid line) as a function of the gravimetric index of the hydrogen storage. For comparison, the ESPG weight of the kerosene-based configuration is also shown (dashed line). A sensitivity analysis was conducted on the gravimetric storage density, from 2 to 30 wt%.

Figure 4 shows the payload weight required for the hydrogen-based aircraft (solid line) to achieve the same MTOW as the conventional solution. It is worth noting that when GI_{HS} is less than 7.5 wt%, even removing the entire payload results in a hydrogen-powered aircraft weighing more than the kerosene-based alternative. For GI_{HS} above approximately 20 wt%, reducing the payload mass by about half is sufficient to match the MTOW of the kerosene aircraft.

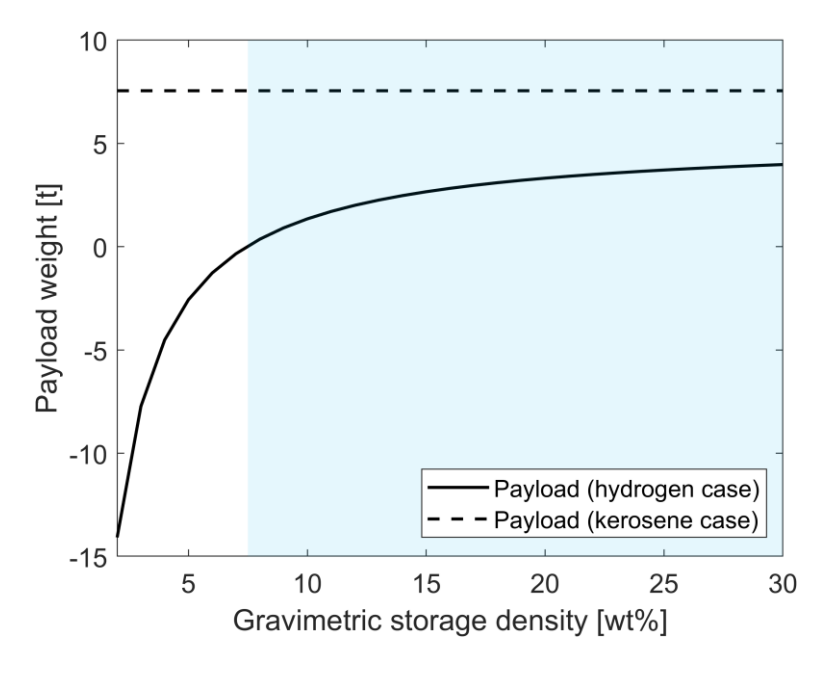


Figure 4 – Payload weight of the hydrogen-based configuration (solid line) to achieve the same MTOW as the kerosene-based aircraft (whose payload weight is shown by the dashed line). A sensitivity analysis was conducted on the gravimetric index of the hydrogen storage.

Currently, the high conversion efficiency of fuel cells cannot compensate for the demanding weight requirements of hydrogen-based propulsion systems. In particular, to render a hydrogen-based

powertrain solution technically feasible, it is essential to further reduce the weight associated with the hydrogen storage and the cooling system. Encouragingly, literature suggests promising values for the gravimetric storage density, e.g. up to 50% for the liquid hydrogen technology, as reported by Massaro et al. [9]. Additionally, the use of a high-temperature PEM fuel cell could help mitigate the weight impact of the cooling unit. In this analysis, the gravimetric power density of the weight-optimal fuel cell system (encompassing fuel cell stacks and related auxiliaries) was computed in the range of 0.8-1.2 kW/kg, depending on the configuration. A system-level value of 2-3 kW/kg is expected in the near future, particularly with the adoption of the high-temperature PEM technology [9], which would make the use of fuel cells in aviation increasingly attractive.

4. Conclusions

The aim of this study was to explore the technical viability of fuel cell-based propulsion systems for aviation. Specifically, the retrofit of a regional aircraft (ATR 72-600) currently powered by kerosene was investigated. To this end, a methodology was developed to perform the weight-optimal design of the energy storage and power generation (ESPG) system. Several configurations were assessed by changing the hydrogen storage typology. Key results can be summarised as follows:

- The weight-optimal number of fuel cell stacks is always higher than the minimum number required. This means that the stack oversizing can effectively enable the fuel cell to operate at points of higher efficiency, resulting in design benefits for both the hydrogen storage and the cooling system.
- The weight-optimal number of fuel cell stacks decreases by increasing the gravimetric storage density. In fact, the weight impact of the hydrogen storage is reduced, making the stack oversizing progressively less effective. On the other hand, the fraction of weight associated with the cooling system increases.
- Currently, the maximum take-off weight (MTOW) of the hydrogen-based aircraft is higher than that of kerosene-fuelled configurations. In order to achieve weight parity with conventional solutions, improvements are needed, particularly in the hydrogen storage and the cooling system. Notably, a sharp reduction in the ESPG weight was found up to a gravimetric storage density of approximately 15 wt%, indicating that values above this threshold should be targeted. Additionally, since the cooling system contributes significantly to the ESPG weight (up to 50%), research should delve into the challenges related to on-board thermal management of fuel cells. In this context, the high-temperature PEM technology represents a promising candidate worth exploring in future studies.

5. Contact Author Email Address

paolo.marocco@polito.it

6. Copyright Statement

The authors confirm that they, and/or their company or organization, hold copyright on all of the original material included in this paper. The authors also confirm that they have obtained permission, from the copyright holder of any third party material included in this paper, to publish it as part of their paper. The authors confirm that they give permission, or have obtained permission from the copyright holder of this paper, for the publication and distribution of this paper as part of the ICAS proceedings or as individual off-prints from the proceedings.

7. Acknowledgements

This publication is part of the project NODES which has received funding from the MUR – M4C2 1.5 of PNRR funded by the European Union - NextGenerationEU (Grant agreement no. ECS00000036).

The authors would like to acknowledge the support provided by Leonardo S.p.A. through the funding of Maria Chiara Massaro's doctoral scholarship and thank the Advanced Power and Energy Systems Research Unit of the Future Aircraft Technologies Leonardo Lab for their collaboration on this topic.

References

- [1] Sacchi R, Becattini V, Gabrielli P, Cox B, Dirnaichner A, Bauer C and Mazzotti M. How to make climate-neutral aviation fly. Nature Communications, Vol. 14, No. 1, pp 1–17, 2023.
- [2] Terrenoire E, Hauglustaine D A, Gasser T and Penanhoat O. The contribution of carbon dioxide emissions from the aviation sector to future climate change. Environmental Research Letters, Vol. 14, No. 8, 2019.
- [3] Baroutaji A, Wilberforce T, Ramadan M and Olabi A G. Comprehensive investigation on hydrogen and

- fuel cell technology in the aviation and aerospace sectors. Renewable and Sustainable Energy Reviews, Vol. 106, pp 31–40, 2019.
- [4] Yusaf T, Faisal Mahamude A S, Kadirgama K, Ramasamy D, Farhana K, A. Dhahad H and Abu Talib A R. Sustainable hydrogen energy in aviation A narrative review. International Journal of Hydrogen Energy, Vol. 52, pp 1026–1045, 2024.
- [5] Schäfer A W, Barrett S R H, Doyme K, Dray L M, Gnadt A R, Self R, O'Sullivan A, Synodinos A P and Torija A J. Technological, economic and environmental prospects of all-electric aircraft. Nature Energy, Vol. 4, pp 160–166, 2019.
- [6] Svensson C, Oliveira A A M and Grönstedt T. Hydrogen fuel cell aircraft for the Nordic market. International Journal of Hydrogen Energy, Vol. 61, pp 650–663, 2024.
- [7] Hoelzen J, Silberhorn D, Zill T, Bensmann B and Hanke-Rauschenbach R. Hydrogen-powered aviation and its reliance on green hydrogen infrastructure Review and research gaps. International Journal of Hydrogen Energy, Vol. 47, No. 5, pp 3108–3130, 2022.
- [8] Peacock J, Cooper R, Waller N and Richardson G. Decarbonising aviation at scale through synthesis of sustainable e-fuel: A techno-economic assessment. International Journal of Hydrogen Energy, Vol. 50, pp 869–890, 2024.
- [9] Massaro M C, Biga R, Kolisnichenko A, Marocco P, Monteverde A H A and Santarelli M. Potential and technical challenges of on-board hydrogen storage technologies coupled with fuel cell systems for aircraft electrification. Journal of Power Sources, Vol. 555, p 232397, 2023.
- [10] Liu H, Qin J, Li C, Li C and Dong P. Performance comparison and potential evaluation of energy systems with different fuel cells for electric aircraft. Applied Thermal Engineering, Vol. 242, p 122447, 2024.
- [11] Schröder M, Becker F and Gentner C. Optimal design of proton exchange membrane fuel cell systems for regional aircraft. Energy Conversion and Management, Vol. 308, p 118338, 2024.
- [12] Massaro M C, Pramotton S, Marocco P, Monteverde A H A and Santarelli M. Optimal design of a hydrogen-powered fuel cell system for aircraft applications. Energy Conversion and Management, Vol. 306, p 118266, 2024.